International Journal of Engineering

Journal Homepage: www.ije.ir

Couple Stress Effect on Micro/Nanocantilever-based Capacitive Gas Sensor

A. M. Abazari *[a], S. M. Safavi[a], G. Rezazadeh[b], M. Fathalilou[b]

[a] *Department of Mechanical Engineering, Isfahan University of Technology, Iran*
[b] *Department of Mechanical Engineering, Urmia University, Iran*

PAPER INFO

Paper history:
Received 23 December 2015
Received in revised form 02 June 2016
Accepted 02 June 2016

Keywords:
Chemical Sensors
Micro Electromechanical Systems
Micro/Nanocantilever
Couple Stress
Resonance Shifting

ABSTRACT

Micro/nanocantilevers have been employed as sensors in many applications including chemical and biosensing. Due to their high sensitivity and potential for scalability, miniature sensing systems are in wide use and will likely become more prevalent in micro/nano-electromechanical systems (M-NEMSs). This paper is mainly focused on the use of sensing systems that employ micro/nano-size cantilever beams for sensing gaseous molecules. Micro/nanocantilever-based gas sensing is concerned with determining the micro/nanocantilever resonance shift or detecting the micro/nanocantilever deflection due to adsorption event. This paper has considered the former approach, i.e., determining the resonance shift. In order to explain these changes more clearly, a micro/nanobeam has to be modeled by considering some micro/nanoscale parameters. A modeling based on classic elasticity theory potentially is unable to consider micro/nanoscale parameters which have considerable effects on the behavior of the micro/nanobeams. The effect of couple stress on the stiffness of cantilever beams remains an outstanding problem in the physical sciences. So in this paper, a modeling based on couple stress theory has been applied to explore the behavior of a micro/nanobeam due to the adsorption of gaseous molecules. This work has attempted to advance the field of micro/nanocantilever based gas sensing by shedding more light on the mechanical behavior of micro/nanocantilever.

***doi**: 10.5829/idosi.ije.2016.29.06c.00*

1. INTRODUCTION

While the results of the elementary theories like the Euler-Bernoulli beam theory and the method of assumed modes do match the experimental results in many situations, both of these theories assume that the constitutive model is independent of length scale (e.g., Hooke's Law). It is realized that additional parameters are needed to relate stress and strain at the [1-4] and describe mechanical properties of micro/nanoscale structures like Young's Modulus [5]. This assumption works well for macro-scale structures, but experimentally, some structures show an increasing resistance to certain deformation modes as the length scale diminishes, a phenomenon neglected by formulations based on the Hooke's. Tortonese and Kirk introduced a static method that involved pressing a test beam against a reference micro/nanocantilever and measuring the deflections of the test beam by applying the optical lever method [6]. The so-called uni-constant elastic theory, which was presented by the Paris Academy [7], is an elementary model based on interatomic potentials and a highly-idealized molecular structure and deformation. Since the model presented in that paper does not consider the length scale, it has found little usage. However, it has provided an important starting point for the classical theory of elasticity. Another well-known theory is the nonlocal elasticity theory, which maintains that the stress at a point is not only a function of the strain at that point but also a function of the strain in a small neighborhood around that point. The important point in this theory is that a neighborhood must be defined by choosing a position vector from the local position that defines the neighborhood space [8, 9]. The general idea of the micro/nanostructural and micro/nanomorphic elasticity theories (presented by Mindlin [10] and Eringen [9], respectively) is that the points of the continuum associated with a micro/nanostructure of finite size can

*Corresponding Author's Email: *abazari@gmail.com* (A.M. Abazari)

Please cite this article as: A. M. Abazari, S. M. Safavi, G. Rezazadeh, M. Fathalilou, Couple Stress Effect on Micro/Nanocantilever-based Capacitive Gas Sensor, International Journal of Engineering (IJE), TRANSACTIONS C: Aspects Vol. 29, No. 6, (June 2016)

deform macroscopically (yielding the classical elasticity case) as well as micro/nanostructurally (producing the length scale effect). The couple-stress concept (the theory used for the modeling in this paper) has been presented by Searle [11]. However, the details of this idea were initially described by the Cosserats. The Cosserat brothers introduced their couple stress theory in 1909, taking into account not only the local translational motion of a point within a material body but also the local rotation of that point [12], and yielded a constitutive model which was nonlinear from the beginning. Some researchers have tried to employ the strain gradient theory in their modeling, which is very similar to the couple stress theories. The strain gradient theory uses the second order deformation gradients but decomposes these gradients into two independent parts: the stretch gradient tensor and the rotation gradient tensor [13, 14]. Recently, some researchers have applied the non-classic theories of elasticity to study the mechanical behavior of electrostatically actuated micro/ nano-beams [15-18]. Rezazadeh et al. [19-21] have studied the application of piezoelectric layers and also the effect of length scale parameter in electrostatic MEMS actuators. Alashti and Abolghasemi [22] investigated a formula for a Euler- Bernoulli beam based on a new model of couple stress theory. Noori and Jomehzadeh [23] used the modified couple stress theory to study vibration analysis of functionally graded rectangular micro-plates.

In this paper, the behavior of a micro/nano-beam under electrostatic actuation is modeled by considering the couple stress theory and then the sensory behavior of the micro/nanocantilever due to the adsorption of an analyte is investigated. This paper has been organized as follows. Section 2 describes in detail the sensory mechanism proposed in this paper and mathematical modeling for the attempted problem is formulated in this Section. The mathematical modeling has separated to four subsections to improve readability of the paper. A numerical method to solve the proposed mathematical model is presented in Section 3. Some benchmark problems adopted from the literature are solved in Section 4 to compare the performance of the proposed numerical method against the existing approaches in the literature. This section is followed by the results of our modeling. Finally, the concluding remarks are presented in Section 5.

2. MATHEMATICAL MODEL

2. 1. Model Description The model consists of a deformable micro/nanocantilever as an electrode and another plate as a stationary base of a micro/nano-capacitor subjected to a voltage (see Figure 1). The length, thickness, width, surface area, cross-sectional moment of inertia, density and Young's modulus of the micro/nanocantilever are represented by L, h, b, A, I, ρ, and E, respectively. The surface of the micro/nanocantilever is coated with a layer which is sensitive to a specific gas (this will be explained in Section 2.3).When the micro/nanocantilever interacts with a gas sample from the environment, a layer-gas molecule complex forms and leads to a change in resonance frequency. In the other hand, the capacitive method [24] is based on the notion that the capacitance of a plane capacitor changes when a cantilever deflects due to the adsorption of gas molecules.

2. 2. Capacitive Force Finding the force between the plates of a standard flat capacitor by ignoring the boundary effects yields the results as a function of constant charge Q, for an isolated capacitor, and as a function of constant voltage V, for a capacitor connected to an ideal voltage generator. In this paper, the term "capacitive force" refers to the electrostatic force generated when a voltage is applied between the plates (deformable cantilever and stationary plate) of a capacitor. The electrostatic pressure is calculated as follows. If A is the surface area of the plates, the surface charge density (on the inner surfaces) will be $\pm\sigma_q = \pm Q/A$ and the uniform field (E*) inside the capacitor will be $E^*=\sigma/\varepsilon_0$. Then the electrostatic pressure can be obtained as:

$$P = \frac{1}{2}\sigma E^* = \frac{\sigma^2}{2\varepsilon_0} \quad (1)$$

Since the electrostatic pressure is normal to the charged inner surfaces, force F_c is an attractive force and is given as a function of Q by:

$$F_c = PA = \frac{(Q/A)^2}{2\varepsilon_0}A = \frac{Q^2}{2\varepsilon_0 A} \quad (2)$$

Written as a function of Q, F_c is independent of the distance d between the plates. It is necessary to have this force in terms of distance d. So, Q is replaced by V via Q = CV, where $C = \varepsilon_0 A/d$. Thus:

$$F_c = \frac{(CV)^2}{2\varepsilon_0 A} = \frac{\varepsilon_0 V^2 A}{2d^2} \quad (3)$$

In this equation, $\varepsilon_0 = 8.854\times10^{-12} C^2 N^{-1} m^{-2}$ is the permittivity of vacuum within a gap and V is the applied electrostatic voltage.

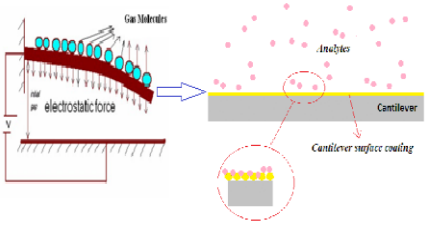

Figure 1. The deflection inducedin a micro/nano-capacitor by the adsorbed gas molecules

2. 3. Adsorption Process Modeling By coating the surfaces of a micro/nanocantilever with an appropriate layer to which an analyte could be attracted, the existing analyte in the surrounding environment would form a bond with that layer. For example, if the surfaces of a micro/nanocantilever are coated (using an electron beam evaporator, for example) with a layer of gold (which is attractable to thiol), a gold-thiolate bond would form upon the adsorption of thiol.

If the adsorption surface area of a layer for an analyte (which is known for some analyte-layers; for example, thiol is known to self-assemble on gold surfaces forming a dense, closely packed monolayer, and taking up 0.21 nm^2 of surface area per molecule [25-27]) is $A_{adsorption}$, the number of molecules that could be adsorbed on that layer can be calculated as:

$$N_{Molecules} = \frac{A_{Layer}}{A_{Adsorption}} \quad (4)$$

where A_{Layer} is the surface area of the layer that could be exposed to an analyte and adsorb its molecules. Knowing the surface area of the layer and the molecular weight of the molecules bonded with it, the adsorbed mass of a perfect monolayer is determined from:

$$m_{added} = M_{Molecular} \times N_{Molecules} = \frac{M_{Molar}}{N_{Avogadro}} \times \frac{A_{Layer}}{A_{Adsorption}} \quad (5)$$

where $M_{Molecular}$, M_{Molar} and $N_{Avogadro}$ are the mass of one molecule, the molar mass of the analyte and the Avogadro's number, respectively.

2. 4. Mechanical Modeling Considering Couple Stress Effect In order to investigate the mechanical behavior of a micro/nanocantilever due to the electrostatic force and the presence of gas molecules, the Euler-Bernoulli assumptions are used. The governing differential equation for the deflection of the cantilever is fully described in this section.

A schematic of the proposed structures is shown in Figure 2. The upper beam is a cantilever. The structure is electrostatically actuated over an initial ideally-uniform gap that changes to a position-dependent gap d by increasing the DC bias voltage between the fixed-ground conductor and the conducting deformable structure with an ideally-fixed end. When a voltage is applied between the upper and lower electrodes, the upper deformable beam is pulled down due to the electrostatic force. The static pull-in voltage is determined by coupling the mechanics to a nonlinear voltage dependent electrostatic pressure term and finding the lowest voltage at which the system is unstable.

Two-dimensional Euler-Bernoulli beam bending theory is employed here to model the mechanics of the assumed structure. This theory considers the following

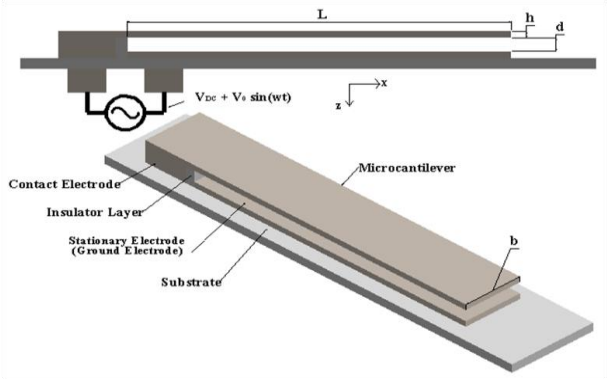

Figure 2. An electrostatically-actuated micro/nanocantilever

assumptions (These assumptions are valid for typical vertically-actuated MEMS geometries which have large in-plane dimensions relative to their thicknesses and gaps):

- Small deflections for which the radius of curvature equals the inverse of the second derivative of deflection,
- No shear deformation due to transverse loading,
- No in-plane (longitudinal, width-wise or radial) curvature adjustments due to the transverse (vertical) extension or contraction of the thickness resulting from a transverse (vertical) load,
- The anticlastic curvature along a beam's width (b) is geometrically insignificant, but the plate-like changes in stiffness, as w increases, can be modeled by adjusting the effective modulus,
- The supports are ideally fixed and
- A uniform initial gap of g_o exists in the unloaded state.

Now, it is time to introduce the governing equation for the beam illustrated in Figure 2, by considering the couple stress effects. Considering the coordinate system (x, z) shown in Figure 2, the x-axis coincides with the centroidal axis of the undeformed beam and the z-axis is the axis of symmetry. In the linear couple stress theory, the strain energy of a deformed body is assumed to depend on strain $\boldsymbol{\varepsilon}$ and rotation gradient $\boldsymbol{\kappa}$, so that the associated stress includes the symmetric Cauchy stress tensor $\boldsymbol{\sigma}$ and the deviatoric couple stress tensor $\boldsymbol{\mu}$ [3]. Consequently, the strain energy E_s in a deformed isotropic linearly elastic material occupying region V is expressed as:

$$E_s = \frac{1}{2}\iiint_V (\boldsymbol{\sigma} : \boldsymbol{\varepsilon} + \boldsymbol{\mu} : \boldsymbol{\kappa}) dv \quad (6)$$

In addition, the kinetic energy of a body in motion is obtained as follows:

$$E_k = \frac{1}{2}\int_V \rho \dot{\boldsymbol{u}}.\dot{\boldsymbol{u}} dv \quad (7)$$

where $\dot{\boldsymbol{u}}$ is the velocity vector. The constitutive equations of the theory are derived by considering the following expression for the strain energy density e_s [28]:

$$e_s = \frac{1}{2}\lambda(\mathrm{tr}\varepsilon)^2 + \mu\varepsilon:\varepsilon + 2\eta\boldsymbol{\kappa}:\boldsymbol{\kappa} + 2\eta'\boldsymbol{\kappa}:\boldsymbol{\kappa}^T \tag{8}$$

where λ and μ are two Lame's constants of the classical elasticity, whereas η and η' are two non-classical Lame-type material constants which introduce the couple stress effects. Equation (8) leads to the following constitutive equations:

$$\boldsymbol{\sigma} = \frac{\partial e_s}{\partial \boldsymbol{\varepsilon}} = \lambda \mathbf{I}:\boldsymbol{\varepsilon} + 2\mu\boldsymbol{\varepsilon}$$
$$\boldsymbol{\mu} = \frac{\partial e_s}{\partial \boldsymbol{\kappa}} = 4\eta\boldsymbol{\kappa} + 4\eta'\boldsymbol{\kappa}^T \tag{9}$$

The displacement components of a Euler-Bernoulli beam, disregarding the mid-point displacement in the x direction, can be expressed as [29]:

$$u = -z\frac{\partial w}{\partial x},\ v = 0,\quad w = w(x,t) \tag{10}$$

where *u*, *v* and *w* are the *x*, *y* and *z* components of the displacement vector, respectively. In view of Equation (10), the components of the symmetric strain tensor for the plane strain conditions are as follows:

$$\varepsilon_{xx} = \frac{\partial u}{\partial x} = -z\frac{\partial^2 w}{\partial x^2}$$

Plane strain: (11)

$$\varepsilon_{yy} = 0,\ \varepsilon_{zz} = \frac{\nu}{(1-\nu)}z\frac{\partial^2 w}{\partial x^2},\ \varepsilon_{xy} = \varepsilon_{yz} = \varepsilon_{zx} = 0$$

where ν is the Poisson's ratio of the cantilever material. The components of the rotation vector can be written as:

$$\theta_y = -\frac{\partial w}{\partial x},\quad \theta_x = \theta_z = 0 \tag{12}$$

Now, the components of the asymmetric rotation-gradient tensor are found as:

$$\kappa_{xy} = -\frac{\partial^2 w}{\partial x^2}$$
$$\kappa_{xx} = \kappa_{yy} = \kappa_{zz} = \kappa_{yx} = \kappa_{xz} = \kappa_{zx} = \kappa_{zy} = \kappa_{yz} = 0 \tag{13}$$

By substituting Equation (11) and Equation (13) into Equation (9) the following relation is obtained for strain energy density in plane strain conditions:

$$e_s = \frac{1}{2}\bar{E}\left(\frac{\partial u}{\partial x}\right)^2 + 2\eta\left(\frac{\partial^2 w}{\partial x^2}\right)^2 \tag{14}$$

$\bar{E}$ is the elastic modulus of the material in plane strain conditions, and can be obtained from:

$$\bar{E} = \frac{E}{1-\nu^2} = \lambda\left(\frac{1-2\nu}{1-\nu}\right)^2 + 2G\left(1+\left(\frac{\nu}{1-\nu}\right)^2\right) \tag{15}$$

where G is the shear modulus of the material. Considering the equation (14), if the width of a beam (b) is equal to or greater than five times of its thickness (h), i.e.,b≥5h, the plain strain condition will be satisfied (the beam in this situation will be called a wide beam) and $\bar{E} = E/1-\nu^2$; but if b< 5h then $\bar{E} = E$. As is indicated by Equation (14), the strain energy in the considered beam model does not depend on η', and only one non-classical material constant appears in this model, which is defined as [3]:

$$\eta = Gl^2 \tag{16}$$

where *l* is the material length scale parameter [28-30].

2. 5. Universal Model Considering the mentioned equations in Sections 2. 2, 2. 3 and 2. 4, and applying the Hamilton principle, the following governing vibration equation is obtained for the cantilever:

$$\left(\bar{E}I + 4GAl^2\right)\frac{\partial^4 w}{\partial x^4} + \left(\rho A + m_{added}\right)\frac{\partial^2 w}{\partial t^2} = F_c^* \tag{17}$$

with the following boundary conditions:

$$w = \frac{\partial w}{\partial x} = 0 \text{ at } x = 0$$

and (18)

$$\frac{\partial^2 w}{\partial x^2} = \frac{\partial^3 w}{\partial x^3} = 0 \text{ at } x = L$$

In Equation (17), F^*_c and m_{added} are the electrostatic force and the added mass, which are respectively calculated by Equation (3) and Equation (5) divided by *L*(the length of the beam) to make the equation dimensionally compatible, and *d* is the total distance between the capacitor plates. Because of the electrostatic force generated by the applied voltage and the deflection of the upper beam towards the lower stationary beam, the total distance between the beams will be $d=g_0-w$. Where, g_0 is the initial gap between the beams. So the F^*_c and m_{added} values will be updated as:

$$F_c^* = \frac{\varepsilon_0 b V^2}{2(g_0 - w)^2},\quad m_{added} = \frac{M_{Molecular} \times N_{Molecules}}{L} \tag{19}$$

Equation (17) can be converted into a non-dimensional form, for convenience.

So, the transverse displacement, w, and the spatial coordinate, x, are respectively normalized by the characteristic lengths of the system, i.e., the initial gap size and beam length, according to: $\hat{w} = w/g_0$ and $\hat{x} = x/L$. Time t in the non-dimensional form is expressed as: $\hat{t} = t/t^*$ where $t^* = (\rho bhL^4 / \bar{E}I)^{1/2}$ is the classical characteristic fundamental period of the system. By substituting these parameters into Equation (17), the following non-dimensional equation is obtained:

$$(1+\alpha)\frac{\partial^4 \hat{w}}{\partial \hat{x}^4} + (1+\beta)\frac{\partial^2 \hat{w}}{\partial \hat{t}^2} = \frac{\gamma V^2}{(1-\hat{w})^2}$$
$$\alpha = \frac{48\mu l^2}{\bar{E}h^2},\ \beta = \frac{m_{added}}{\rho A},\ \gamma = \frac{6\varepsilon_0 L^4}{\bar{E}h^3 {g_0}^3} \quad (20)$$

3. NUMERICAL SOLUTION

In the numerical solution, it is assumed that a DC voltage, V_s, deflects the micro/nanocantilever and then the dynamic motions of the system are analyzed by considering these conditions. Thus, the total deflection of the micro/nanocantilever consists of the following two parts:

$$\hat{w}(\hat{x},\hat{t}) = \hat{w}_s(\hat{x}) + \hat{w}_d(\hat{x},\hat{t}) \quad (21)$$

$\hat{w}_s(\hat{x})$ is the static deflection of the cantilever and $\hat{w}_d(\hat{x},\hat{t})$ is the dynamic deflection about the $\hat{w}_s(\hat{x})$. For getting the pull-in voltage of the system, the cantilever's static deflection should be calculated, and then Equation (17) should be used to obtain the frequency response.

3. 1. Static Deflection The static equation can be derived by removing the time-dependent term from the dynamic equation of motion (Equation (20)) as follows:

$$(1+\alpha)\frac{\partial^4 \hat{w}_s}{\partial \hat{x}^4} = \frac{\gamma V_s^2}{(1-\hat{w}_s)^2} \quad (22)$$

Due to the nonlinearity of the derived static equation, direct application of either the Galerkin method or the finite difference method will produce a set of nonlinear algebraic equations. To avoid this problem, the step-by-step linearization method (SSLM) [31] is applied followed by the Galerkin method to linearize and solve the obtained linear set of algebraic equations. For using the SSLM, it is assumed that $\hat{w}_s^k$ is the displacement of the beam due to the applied voltage V^k. It is supposed that $\hat{w}^k$ is the non-dimensional displacement of the micro/nanostructure when subjected to V^k. Then, with a small increase in the voltage, the deflection of the $(k+1)^{th}$ step can be obtained as:

$$V^{k+1} = V^k + \delta V \ \ \& \ \ \hat{w}^{k+1} = \hat{w}^k + \delta\hat{w} = \hat{w}^k + \psi \quad (23)$$

where δV is the voltage change between two successive steps. By considering a small δV value, ψ will be small enough so that the first term of the Taylor expansion in each step could be used instead of the whole main excitation function. The equation for the k^{th} step is:

$$(1+\alpha)\left.\frac{d^4\hat{w}}{d\hat{x}^4}\right|_k = \frac{\gamma (V^k)^2}{(1-\hat{w}^k)^2} \quad (24)$$

and for the $(k+1)^{th}$ step we have:

$$(1+\alpha)\left.\frac{d^4\hat{w}}{d\hat{x}^4}\right|_{k+1} = \frac{\gamma (V^{k+1})^2}{(1-\hat{w}^{k+1})^2} \quad (25)$$

Based on the Calculus of Variation Theory, and using the Taylor's expansion series, the second part of Equation (25) can be written as:

$$\frac{\gamma (V^{k+1})^2}{(1-\hat{w}^{k+1})^2} = \frac{\gamma (V^k)^2}{(1-\hat{w}^k)^2} + \frac{2\gamma (V^k)^2}{(1-\hat{w}^k)^2}\delta V + \frac{2\gamma (V^k)^2}{(1-\hat{w}^k)^3}\psi \quad (26)$$

By substituting Equation (26) into Equation (25) and then subtracting Equation (25) from Equation (24) and considering Equation (23) we get:

$$(1+\alpha)\frac{d^4\psi}{d\hat{x}^4} - \left(\frac{2\gamma (V^k)^2}{(1-\hat{w}^k)^3}\right)\psi = \delta V \frac{2\gamma V^k}{(1-\hat{w}^k)^2} \quad (27)$$

Now, the obtained linear differential equation can be solved by the Galerkin method. Based on the function space, $\psi(\hat{x})$ may be expressed as:

$$\psi(\hat{x}) = \sum_{j=1}^{\infty} a_j \phi_j(\hat{x}) \quad (28)$$

$\phi_j(\hat{x})$ is the j^{th} shape function which satisfies the given boundary conditions. In this paper, the shape functions are selected as the linear undamped natural mode shapes of the beam. The unknown $\psi(\hat{x})$ is approximated by truncating the summation series to a finite number, n:

$$\psi_n(\hat{x}) = \sum_{j=1}^{n} a_j \phi_j(\hat{x}) \quad (29)$$

By substituting Equation (29) into Equation (27), multiplying the resulting equation by $\phi_j(\hat{x})$ (a weight function in the Galerkin method) and integrating the outcome from $\hat{x} = 0$ to 1 a set of linear algebraic equations is generated as:

$$\sum_{j=1}^{n} K_{ij} a_j = F_i \quad , \quad i = 1,\ldots,n \tag{30}$$

where:

$$K_{ij} = \int_0^1 \phi_i \left[(1+\alpha)\phi_j^{iv} - 2\gamma \frac{\left(V^k\right)^2}{\left(1-\hat{w}_s^k\right)^3} \phi_j \right] d\hat{x}$$
$$F_i = \int_0^1 \phi_i \left[2\gamma \frac{V^k}{\left(1-\hat{w}_s^k\right)^2} dV \right] d\hat{x} \tag{31}$$

In Equation (31), K_{ij} represents the stiffness of the micro/nanocantilever.

3. 2. Dynamic Deflection The dynamic loading response could be obtained by using a Galerkin-based reduced order model. The procedure is the same as that for static deflection. However, here, the time dependent term should be considered as well. In addition, the voltage in this mode of deflection will be $V = V_s + V_0 \sin(\Omega t)$. First, a static voltage (V_s) is applied, then, by applying a harmonic voltage ($V_0 \sin(\Omega t)$) with frequency Ω, the beam is forced to oscillate at the frequency of the applied force. Since in this model, the applied AC voltage is much smaller than the DC voltage ($V_{AC} << V_{DC}$), by linearizing Equation (20) in terms of the calculated $\hat{w}_s(\hat{x})$, the small linear vibrations could be obtained by the following equation:

$$(1+\alpha)\frac{\partial^4(\hat{w}_s+\hat{w}_d)}{\partial\hat{x}^4} + (1+\beta)\frac{\partial^2\hat{w}_d}{\partial\hat{t}^2} = \gamma\frac{V_s^2}{(1-\hat{w}_s)^2} + 2\gamma\frac{V_s}{(1-\hat{w}_s)^2}\delta V + 2\gamma\frac{V_s^2}{(1-\hat{w}_s)^3}\delta\hat{w} \tag{32}$$

here, $\delta V = V_0 \sin(\Omega t)$ and $\delta\hat{w} = \hat{w}_d$. By subtracting Equation (22) from Equation (32), the linearized equation of motion about the equilibrium position can be obtained as:

$$(1+\alpha)\frac{\partial^4\hat{w}_d}{\partial\hat{x}^4} + (1+\beta)\frac{\partial^2\hat{w}_d}{\partial\hat{t}^2} - \frac{2\gamma V_s^2}{(1-\hat{w}_s)^3}\hat{w}_d = \frac{2\gamma V_s V_0 \sin(\Omega t)}{(1-\hat{w}_s)^2} \tag{33}$$

To achieve a reduced order model, $\hat{w}(\hat{x},\hat{t})$ may be approximated as:

$$\hat{w}(\hat{x},\hat{t}) = \sum_{j=1}^{n} T_j(\hat{t})\phi_j(\hat{x}) \tag{34}$$

By substituting Equation (34) into Equation (20), multiplying the resulting equation by $\phi_i(\hat{x})$ (as a weight function in the Galerkin method) and integrating the outcome from $\hat{x} = 0$ to 1, the Galerkin-based reduced order model is generated as:

$$\sum_{j=1}^{n} M_{ij}\ddot{T}_j(\hat{t}) + \sum_{j=1}^{n} K_{ij} T_j(\hat{t}) = F_i \sin(\Omega t) \tag{35}$$

Where M and K are the mass and mechanical stiffness matrices, respectively. In addition, F introduces a force vector. The mentioned matrices and the vector are expressed as:

$$M_{ij} = (1+\beta)\int_0^1 \phi_i\phi_j d\hat{x}$$
$$K_{ij} = (1+\alpha)\int_0^1 \phi_i\phi_j^{iv} d\hat{x} - \frac{2\gamma V_s^2}{(1-w_s)^3}\int_0^1 \phi_i\phi_j d\hat{x} \tag{36}$$
$$F_i = \frac{2\gamma V_s V_0}{(1-w_s)^2}\int_0^1 \phi_i d\hat{x}$$

Now, Equation (35) can be integrated over time by various integration methods such as the Runge-Kutta method.

4. RESULTS AND DISCUSSION

4. 1. Numerical Method Validation For the validation of the numerical solution, the micro/nano-beam investigated by Osterberg [32] with its geometrical properties shown in Table 1 has been considered and to be able to compare the result, the length scale parameter has been considered as zero. Table 1 indicates that the calculated pull-in voltage is in good agreement with those in the previous works. Figure 3 illustrates the relevant pull-in voltages obtained by the model proposed in this paper.

After considering the couple stress effect, the pull-in voltage shifts to 18.7, 29.5 and 66.5 when l is taken as 0.1, 0.3 and 0.8h, respectively. The couple stress effect is going to be discussed in detail in the following subsections.

4. 2. Static Behavior of the Sensor To compare a model included couple stress effect with the classical model, the physical parameters of the micro/nanocantilever are considered to have the following values: L= 100, b= 20, h= 2, d= 1 μm, ρ =2331 kg/m3 and ν =0.06.

TABLE 1. Pull-in voltages, V_{PI} (V), for micro/nano-cantilevr with properties:
E = 169(GPa), ν = 0.06, b = 50(μm), h = 3(μm) & d = 1(μm)

	VPI (Proposed Model)	CoSolve simulation [32]	Closedform 2D model [32]
L=150(μm)	16.9	16.9	16.8

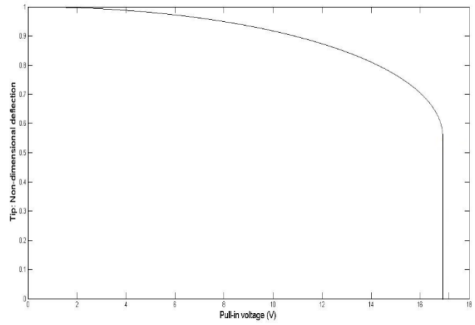

Figure 3. Pull-in voltage for an electrostatically-actuated fixed-fixed micro/nano-beam

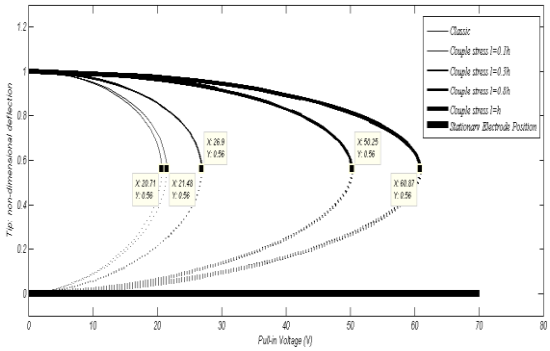

Figure 4. Pull-in voltages for the cantilever-based sensor

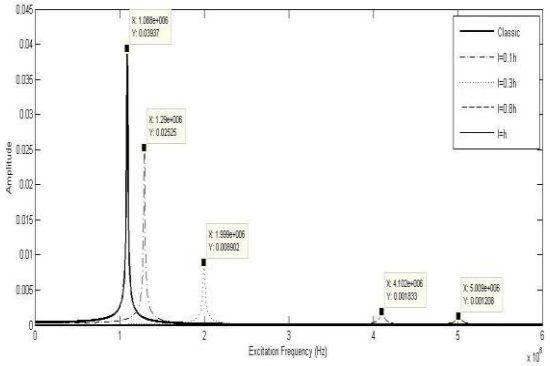

Figure 5. Frequency responses for the classic model and the non-classical models with l=0.1, 0.3, 0.8 and 1.0h

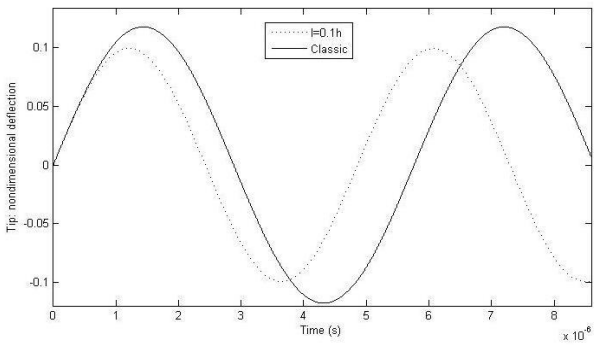

Figure 6. Time-history curves for the classical model and the non-classical model with l=0.1h

Figure 4 shows the effect of couple stress on sensor behavior in the static mode. According to this Figure, the pull-in voltage without considering the couple stress effect (i.e., in the classical model) is lower than the situation while couple stress is considered. It is observed that by increasing the length scale of the material, the pull-in voltage shifts to higher values. Figure 4 reveals that for every voltage, two physically possible tip deflection values exist. The regions outlined by dashed lines are the regions in which the cantilever is unstable; in other words, if the deflection of the cantilever reaches these regions, the system will collapse and the cantilever will touch the lower plate.

4. 3. Dynamic Behavior of the Sensor Figure 5 demonstrates the effect of couple stress on sensor behavior in the dynamic mode. It is shown in this Figure that, as expected, the resonance frequency without considering the couple stress effect (i.e., in the classical model) is lower than the situation while couple stress effect is considered. It is shown that increasing the length scale of the material leads to a higher resonance frequency. These results are in complete agreement with the results of the static mode analysis.

In Figure 6, the time history curves of the free vibrations have been plotted for the cases which consider classical model (l=0) and non-classical model with l=0.1× h. It is evident that with consideration of the couple stress effect, the vibration frequency is increased and the vibration amplitude is reduced.

In view of Figures 5 and 8, it is easy to see that there is a difference between the classical model and the case which considers the length scale as a design parameter. After realizing that the length scale parameter should be taken into consideration when designing micro/nanoscale structures, it is now time to test the proposed model by exposing the system to gaseous molecules.

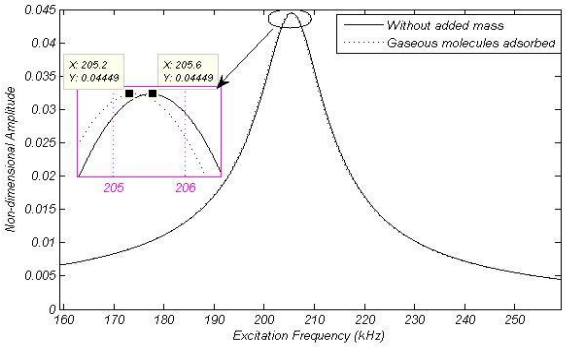

Figure 7. Shifting of resonance frequency due to the adsorption of gas molecules

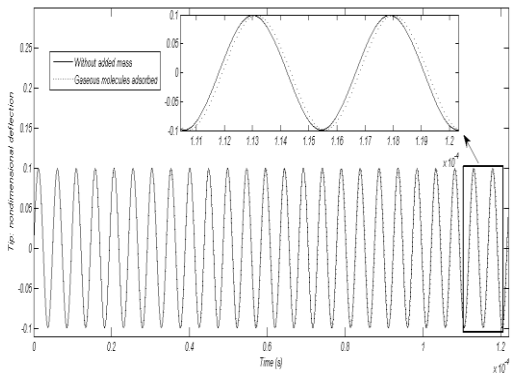

Figure 8. Time-history cureves

In the following section, the adsorption of gaseous molecules on the beam surface and its effects on the response and behavior of the beam will be investigated. To make the results easier to illustrate, the length scale parameter considered to be 0.1×h.

4. 4. Sensing Behavior of the Cantilever For investigating the sensing behavior of the proposed model, the surface of the cantilever is assumed to be coated with gold, which has a high affinity to thiol molecules. As was mentioned in Section 2.3, thiols are known to self-assemble on gold surfaces, forming a dense, closely packed monolayer (about 0.21 nm^2 of surface area per molecule [25-27]). Since the area of the gold surface and the molecular weight of the molecules bonded to it are known, the adsorbed mass of a perfect monolayer could be easily calculated by Equation (5) presented in Section 2.3. As a case study, Methane thiol (CH_4S), which is a colorless, flammable and highly toxic gas with a boiling point of 5.95 ºC, is considered here. The adsorbed mass of a perfect monolayer for this gas on the cantilever mentioned in Section 4.2 is approximately 2.1225×10^{-14}kg . It is also assumed that the monolayer itself will not significantly increase the structural stiffness of the micro/nanocantilever.

The natural frequency shift due to the added mass of the adsorbed gaseous molecules (2.1225e-14 kg) is illustrated in Figure 7. Having these plots and calibrating the system, the amount of adsorbed gaseous molecules on a micro/nanobeam can be determined. According to the Figure, the resonance frequency of the sensor, shifts as gaseous molecules are adsorbed on the cantilever surface. As depicted in the Figure, the resonance frequency shift due to the adsorption of gas molecules is roughly 400 Hz.

A complete time-history diagram will indicate the response of a structure over time during and after the application of a load. Here, in Figure 8, the time-history of the relevant sensor before and after the adsorption of gaseous molecules has been plotted. As is shown in this Figure, the adsorption of gaseous molecules on the cantilever surface has led to a reduction in vibration frequency. This Figure confirms the results obtained from the frequency response curve.

5. CONCLUSION REMARKS

As crucial devices for various gas control tasks, gas sensors, will continue to evolve and be in high demand in the future. In this regard, particularly the M-NEMS-based gas sensors need to be further innovated. The sensors of this class have been developed successfully, mostly on empirical bases, thanks to the excellent sensing devices that have been fabricated in various groups; however, further developments seem to be hampered by a lack of theoretical support. This research has revealed the importance of length scale parameter in micro/nano-scale beams which are used in gas sensing industry.

In this paper, the static and dynamic responses of an electrostatically-actuated cantilever-based sensor considering couple stress theory were studied. The responses of micro/nanocantilever due to the adsorption of gaseous molecules were investigated. The calculated static pull-in voltages were validated by the results of previous works. It is shown that the length scale parameter plays an essential role in determining the stiffness of the cantilever which is widely used in the gas sensor. Finally, the frequency response and the time-history behavior of the sensor are investigated with the new model.

The effect of couple stress on the stiffness of cantilever beams remains an outstanding problem in the physical sciences from an experimental point of view. The physical parameters of the structure material (grain size and grain shape which can probably give a more realistic length scale parameter for a material) could be further investigated in future works. Besides, further investigations could be carried out to develop a theory that deals with the receptor function of these sensors.

6. REFERENCE

1. Toupin, R. A., "Elastic materials with couple-stresses", ***Archive for Rational Mechanics and Analysis***, Vol. 11, No. 1, (1962), 385-414.
2. Mindlin, R. and Tiersten, H., "Effects of couple-stresses in linear elasticity", ***Archive for Rational Mechanics and Analysis***, Vol. 11, No. 1, (1962), 415-448.
3. Mindlin, R. D., "Micro-structure in linear elasticity", ***Archive for Rational Mechanics and Analysis***, Vol. 16, No. 1, (1964), 51-78.
4. Koiter, W., "Couple-stresses in the theory of elasticity, i & ii", (1969).
5. Abazari, A. M., Safavi, S. M., Rezazadeh, G. and Villanueva, L. G., "Modelling the size effects on the mechanical properties of micro/nano structures", ***Sensors***, Vol. 15, No. 11, (2015), 28543-28562.

6. Tortonese, M. and Kirk, M., "Characterization of application-specific probes for SPMS", in Photonics West'97, International Society for Optics and Photonics, Vol. 3009, (1997), 53-60.
7. Malvern, L. E., "Introduction to the mechanics of a continuous medium, ***Prentice-Hall***, (1969), 280-296.
8. Mohr, J., "Liga: A technology for fabricating microstructures and microsystems", ***Sensors and Materials***, Vol. 10, No. 6, (1998), 363-373.
9. Eringen, A. C., "Mechanics of micromorphic continua", Springer, (1968).
10. Mindlin, R., "Stress functions for a cosserat continuum", ***International Journal of Solids and Structures***, Vol. 1, No. 3, (1965), 265-271.
11. Searle, G. F. C., "Experimental elasticity: A manual for the laboratory", University Press, (1908).
12. Cosserat, E. and Cosserat, F., "Théorie des corps déformables", ***Paris***, Vol. 3, (1909), 17-29.
13. Fleck, N. and Hutchinson, J., "Strain gradient plasticity", ***Advances in Applied Mechanics***, Vol. 33, (1997), 296-361.
14. Fleck, N. and Hutchinson, J., "A reformulation of strain gradient plasticity", ***Journal of the Mechanics and Physics of Solids***, Vol. 49, No. 10, (2001), 2245-2271.
15. Asghari, M., Ahmadian, M., Kahrobaiyan, M. and Rahaeifard, M., "On the size-dependent behavior of functionally graded micro-beams", ***Materials & Design***, Vol. 31, No. 5, (2010), 2324-2329.
16. Fu, Y. and Zhang, J., "Size-dependent pull-in phenomena in electrically actuated nanobeams incorporating surface energies", ***Applied Mathematical Modelling***, Vol. 35, No. 2, (2011), 941-951.
17. Kong, S., Zhou, S., Nie, Z. and Wang, K., "Static and dynamic analysis of micro beams based on strain gradient elasticity theory", ***International Journal of Engineering Science***, Vol. 47, No. 4, (2009), 487-498.
18. Kong, S., Zhou, S., Nie, Z. and Wang, K., "The size-dependent natural frequency of bernoulli–euler micro-beams", ***International Journal of Engineering Science***, Vol. 46, No. 5, (2008), 427-437.
19. Rezazadeh, G., Tahmasebi, A. and Zubstov, M., "Application of piezoelectric layers in electrostatic mem actuators: Controlling of pull-in voltage", ***Microsystem Technologies***, Vol. 12, No. 12, (2006), 1163-1170.
20. Ghader, R. and Ahmadali, T., "Eliminating of the residual stresses effect in the fixed-fixed end type mems switches by piezoelectric layers", ***Sensors & Transducers Magazine***, Vol. 66, No. 4, (2006), 534-542.
21. Rashvand, K., Rezazadeh, G. and Madinei, H., "Effect of length-scale parameter on pull-in voltage and natural frequency of a micro-plate", ***International Journal of Engineering***, Vol. 27, No. 3, (2014), 375-384.
22. Alashti, R. A. and Abolghasemi, A., "A size-dependent bernoulli-euler beam formulation based on a new model of couple stress theory", ***International Journal of Engineering-Transactions C: Aspects***, Vol. 27, No. 6, (2013), 951-960.
23. Noori, H. and Jomehzadeh, E., "Length scale effect on vibration analysis of functionally graded kirchhoff and mindlin micro-plates", ***International Journal of Engineering Transications C: Aspects***, Vol. 27, (2014), 528-536.
24. Blanc, N., Brugger, J., De Rooij, N. and Durig, U., "Scanning force microscopy in the dynamic mode using microfabricated capacitive sensors", ***Journal of Vacuum Science & Technology B***, Vol. 14, No. 2, (1996), 901-905.
25. Bain, C. D., Evall, J. and Whitesides, G. M., "Formation of monolayers by the coadsorption of thiols on gold: Variation in the head group, tail group, and solvent", ***Journal of the American Chemical Society***, Vol. 111, No. 18, (1989), 7155-7164.
26. Bain, C. D., Troughton, E. B., Tao, Y. T., Evall, J., Whitesides, G. M. and Nuzzo, R. G., "Formation of monolayer films by the spontaneous assembly of organic thiols from solution onto gold", ***Journal of the American Chemical Society***, Vol. 111, No. 1, (1989), 321-335.
27. Bain, C. D. and Whitesides, G. M., "Formation of monolayers by the coadsorption of thiols on gold: Variation in the length of the alkyl chain", ***Journal of the American Chemical Society***, Vol. 111, No. 18, (1989), 7164-7175.
28. Georgiadis, H. and Velgaki, E., "High-frequency rayleigh waves in materials with micro-structure and couple-stress effects", ***International Journal of Solids and Structures***, Vol. 40, No. 10, (2003), 2501-2520.
29. Park, S. and Gao, X., "Bernoulli–euler beam model based on a modified couple stress theory", ***Journal of Micromechanics and Microengineering***, Vol. 16, No. 11, (2006), 2355-2359.
30. Anthoine, A., "Effect of couple-stresses on the elastic bending of beams", ***International Journal of Solids and Structures***, Vol. 37, No. 7, (2000), 1003-1018.
31. Rezazadeh, G., Fathalilou, M. and Sadeghi, M., "Pull-in voltage of electrostatically-actuated microbeams in terms of lumped model pull-in voltage using novel design corrective coefficients", ***Sensing and Imaging: An International Journal***, Vol. 12, No. 3-4, (2011), 117-131.
32. Osterberg, P., "Electrostatically actuated microelectromechanical test structures for material property measurement", Massachusetts Institute of Technology, (1995).

Couple Stress Effect on Micro/Nanocantilever-based Capacitive Gas Sensor

A. M. Abazari [a], S. M. Safavi[a], G. Rezazadeh[b], M. Fathalilou[b]

[a] *Department of Mechanical Engineering, Isfahan University of Technology, Iran*
[b] *Department of Mechanical Engineering, Urmia University, Iran*

P A P E R I N F O

Paper history:
Received 23 December 2015
Received in revised form 02 June 2016
Accepted 02 June 2016

Keywords:
Chemical Sensors
Micro Electromechanical Systems
Micro/Nanocantilever
Couple Stress
Resonance Shifting

چکیده

میکروتیرهای یک‌سرگیردار بعنوان حسگر در بسیاری از کاربردهای شیمیایی مورد استفاده قرار می‌گیرند. بعلت حساسیت بالا، سیستم‌های در مقیاس کوچک کاربرد گسترده‌ای را پیدا کرده‌اند. این مقاله به کاربرد سیستم‌های حسگری که با استفاده از میکروتیر یک‌سرگیردار به منظور شناسایی مولکول‌های گاز مورد استفاده قرار می‌گیرند، می‌پردازد. این سیستم‌ها با تعیین شیفت فرکانسی و میزان خیز میکروتیر در اثر جذب مولکول‌های گاز بر روی سطح آن کار می‌کنند؛ در این مقاله تعیین شیفت فرکانسی مورد بررسی قرار گرفته است. به منظور تحلیل دقیق‌تر رفتار این سیستم‌ها، میکروتیر بایستی با در نظر گرفتن برخی از پارامترهایی که در مقیاس میکرو تاثیر گذار هستند، مدلسازی شود. مدل‌های بر پایه‌ی تئوری‌های کلاسیک، قابلیت در نظر گرفتن این پارامترها را که در مقیاس میکرو و نانو بسیار تاثیرگذار هستند، ندارند. اثر تنش کوپل روی سفتی میکروتیر پارامتر مهمی است که در کاربرد این نوع حسگرها بایستی در نظر گرفته شود. بنابراین، در این مقاله مدلسازی‌ای با در نظر گرفتن تنش کوپل برای میکروتیر ارایه شده است و رفتار میکروتیر بر پایه‌ی این مدل در اثر جذب گاز مورد مطالعه قرار گرفته است.

***doi**: 10.5829/idosi.ije.2016.29.06c.00*